Available online at www.sciencedirect.com
SCIENCE DIRECT
International Journal of Mass Spectrometry 252 (2006) 117–125
International Journal of Mass Spectrometry
www.elsevier.com/locate/ijms

# Fullerene collisions and clusters of fullerenes

O. Kamalou [a], B. Manil [a], H. Lebius [a], J. Rangama [a], B.A. Huber [a,*], P. Hvelplund [b], S. Tomita [c], J. Jensen [d], H.T. Schmidt [e], H. Zettergren [e], H. Cederquist [e]

[a] *Centre Interdisciplinaire de Recherche Ions Lasers (CIRIL) CEA-CNRS-ENSICAEN, Bd. Henri Becquerel, BP 5133, F-14070 Caen, France*
[b] *Department for Physics and Astronomy, Aarhus University, DK-8000 Aarhus C, Denmark*
[c] *Institute for Applied Physics, University of Tsukuba, Tsukuba, Ibaraki 305-0006, Japan*
[d] *Division of Ion Physics, Angström Laboratory, Uppsala University, Box 534, SE-75121 Uppsala, Sweden*
[e] *Physics Department, Stockholm University, AlbaNova University Center, S-10691 Stockholm, Sweden*

Received 9 December 2005; received in revised form 21 December 2005; accepted 21 December 2005
Available online 20 March 2006

**Abstract**

Electron capture processes were studied in glancing collisions between multiply charged $C_{60}^{q+}$ ions and neutral $C_{60}$ molecules at low collision energies where nuclear stopping dominates the interaction (typical energy: 10 keV; velocity $v = 0.024$ a.u.). In addition, clusters of fullerenes were multiply ionized in collisions with highly charged slow ions and their fragmentation spectra were measured by applying multi-coincidence techniques in a second, separate experiment. Through the first experiment we show that non-fragmenting electron capture collisions do not produce free electrons in $C_{60}^{q+}$–$C_{60}$ collisions ($q = 1$–5), i.e., the cross sections for transfer ionization processes are negligible in this charge state regime. This is in contrast to the case of atomic projectile ions where transfer ionization processes, as e.g., $C^{q+} + C_{60} \rightarrow C^{(q-r)+} + C_{60}^{r+} \rightarrow C^{(q-r+1)+} + C_{60}^{r+} + e^-$, are strong for $q > 2$. These results are rationalized by means of the classical over-the-barrier model for electron transfer between two $C_{60}$ molecules, or between an atomic ion and a $C_{60}$ molecule, where the molecules are modeled as conducting spheres. Further, the same model may also be used as a basis for understanding the present observations of limitations in the maximum numbers of charges, which might be transferred in non-fragmenting $C_{60}^{q+}$–$C_{60}$ collisions ($q/2$ for even $q$ and $(q+1)/2$ for odd $q$) and in $C^{q+}$–$C_{60}$ collision (here up to $q$ charges may be transferred). In the same experiment, we have further measured scattering angles, $\theta$, and energy losses, $\varepsilon$, for the fullerene projectiles in $C_{60}^{q+}$–$C_{60}$ collisions and we have found low values for both $\theta$ and $\varepsilon$, which, however, increase with the number of $C_2$-units lost from the projectile fullerene in electron capture collisions. The critical distances for electron transfer which are deduced from the $C_{60}^{q+}$–$C_{60}$ collision experiment and the Zettergren model are then used to explain the high charge mobility between the individual $C_{60}$ molecules in charged $(C_{60})_n$ van der Waal's clusters of fullerenes, which we observe in the second experiment.


*PACS:* 3470; 3450.Bw; 3640.QV; 3640.Wa

*Keywords:* Fullerene; Collision; Fragmentation

## 1. Introduction

In recent years, collisions between slow *atomic* ions and fullerenes have been studied intensively — usually with focus on electron transfer mechanisms, and/or various processes for ionization and heating of the fullerene and the resulting subsequent fragmentation processes [see for example 1–5]. However, collisions involving *two* complex systems, such as two fullerenes, have been studied to much lesser extents. Shen et al. [6] found that non-fragmenting electron capture is the dominating process and that fragmentation resulting from closer collisions leads to the typical bi-modal distribution of product ions for $C_{60}^{q+}$ ($q = 1$, 2)/$C_{70}^{3+}$–$C_{60}$ collisions in the 100 keV range. At considerably lower collision energies, Campbell et al. [7,8] observed complete fusion of two $C_{60}$ molecules in $C_{60}^{+}$–$C_{60}$ collisions (at center-of-mass energies of around 100 eV). While the complete fusion process was found to be a minor channel, partial fusion with fragmentation were identified as the dominant reaction channels

* Corresponding author.
*E-mail address:* huber@ganil.fr (B.A. Huber).

1387-3806/$ – see front matter © 2006 Elsevier B.V. All rights reserved.
doi:10.1016/j.ijms.2005.12.054

[7,8]. A further interesting aspect is that studies of angular distributions for the scattering of projectile fragments in the same collision system [9], showed indications of a phase transition in the collision complex. A related theoretical study by Knospe and Schmidt [10] indicated the occurrence of collective flow phenomena leading to the emission of small fragment jets at 90° with respect to the $C_{60}^+$ projectile beam for small impact parameter collisions.

The ionization of clusters of fullerenes, $(C_{60})_n$, by charged particle impact has been studied to even lesser extent and to the best of our knowledge there is only one series of such experiments performed up to this date [11–13]. There are, however, a few very interesting and related studies of photoionization of clusters of fullerenes. An example here is the pioneering work by Martin et al. [14] in which it was argued that $(C_{60})_n$ are van der Waal's type clusters as the members with $n = 13$ and 55 fullerenes were shown to be particularly stable. These magic numbers are typical for icosahedral structures, which are known to be the form for other van der Waal's clusters such as those formed by noble gases. More recently, the same group has shown [15,16] that transitions between icosahedral, closed–packed and decahedral structures of $(C_{60})_n$ can occur as functions of cluster temperature and that these transitions are independent of the cluster charge. Support for these interpretations are available in the form of global-minima calculations for $(C_{60})_n$ clusters [17]. Concerning the behavior of mixed clusters of $C_{60}$ and $C_{70}$ fullerenes, Hansen et al. [18] have shown that $C_{60}$ and $C_{70}$ participate in very similar ways in the cluster formation processes and also that binding energies and reactivities are similar for pure, $(C_{60})_n$, and mixed, $[(C_{60})_{n-m}(C_{70})_m]$, clusters of fullerenes. In a very recent study [19] of femtosecond laser interactions with clusters of fullerenes, evidence for fusion products with a number of $C_2$-unit below (fused) $C_{120}$, $C_{180}$, $C_{240}$, and $C_{300}$ was presented.

The electrical communication between different fullerene molecules has been discussed, in particular for the dimer case, in connection with possible future optical and electronic applications [20,21]. In the case of *neutral* van der Waal's type clusters, we expect very low charge mobility and for singly charged rare gas clusters it has been shown that the charge is localized on a small number of atoms. The icosahedral $Ar_{13}^+$ cluster, as an example, is arranged around a linear $Ar_3^+$ core [22]. Recently, charge localization effects have been reported for highly charged Ar clusters [23] as evidenced by the production of highly charged atomic fragments up to charge state seven ($Ar^{7+}$) measured in correlation with $Ar^+$ ions in the fragmentation of multiply charged $(Ar)_n$ clusters.

In the present work, we will discuss results obtained in fullerene (ion)—fullerene collisions and we will then use these results in order to briefly discuss the observed high electrical conductivity in singly and multiply charged clusters of fullerenes, $(C_{60})_n$ and $[(C_{60})_{n-m}(C_{70})_m]$.

## 2. Experiment

The fullerene–fullerene collision experiment is described in more detail elsewhere [24–27] and therefore only a brief description will be given here. Multiply charged fullerene ions are extracted from a 14 GHz ECR ion source, which is operated at very low power (∼4 W) using He as a carrier gas and $C_{60}$ molecules sublimated from an oven. The abundance of small-sized fragments (which may overlap in the mass-to-charge ratio with the selected fullerene projectile) depends on the power producing the discharge and here we are interested in using pure beams of $C_{60}^{2+}$, $C_{60}^{3+}$, $C_{60}^{4+}$, and $C_{60}^{5+}$. In the specific case of $C_{60}^{4+}$, a contamination of $C_{15}^+$ is present at a level of roughly 40% [25]. Here, we will, however, only discuss the collision-induced production of projectile fragments with masses larger than that of $C_{15}$ where this contamination cannot contribute. The projectiles pass a bending magnet and an energy monochromator, which defines the mass-to-charge ratio and the kinetic energy spread to ±2q eV, where $q$ is the charge state of the fullerene projectile. The fullerene ion beam crosses a $C_{60}$ jet effusing from a target oven at a temperature of about 500 °C. The interaction of the ion and neutral beams occurs in the first extraction stage of a linear Wiley–McLaren time-of-flight mass spectrometer, where a continuous electric field is applied. Due to the weakness of this field (50 V/cm), we only detect intact fullerene recoil ions (or fragments), which are released with small momenta from the collision processes. The intact or fragmented projectile ions are slightly deviated in the extraction field. Then they pass an angular-defining aperture, an energy analyzer and finally hit a detector. This detection unit can be rotated around the scattering center. Thus, it is possible to measure angular distributions for a given kinetic energy, or, the energy distributions for a given scattering angle. The recoil and projectile fullerene ions are analyzed with respect to mass, charge, and kinetic energies. These quantities can be measured in coincidence for distant collisions. For collisions with zero momentum transfer, the energy distributions of the projectiles reflect the fragment ion mass (and charge) distributions, as mass and energy are proportional.

In the second experiment, a beam of neutral clusters of fullerenes is produced in a cluster aggregation source [26]. Here, a mixture of $C_{60}/C_{70}$ powder is evaporated in an oven at a temperature of ∼550 °C and aggregation of the vapor into clusters of fullerenes ($(C_{60})_n$ and $[(C_{60})_{n-m}(C_{70})_m]$) occurs by super saturation in a cold He atmosphere (pressure of several mbar, temperature $T$ ∼77 K). The formed neutral clusters pass several differential pumping stages before interacting with a beam of highly charged ions ($Xe^{30+}$). Singly and multiply charged fullerene clusters as well as charged fragments are extracted from the interaction zone perpendicular to the two beams and are analyzed with a linear Wiley–McLaren time-of-flight mass spectrometer. The particles are post-accelerated towards a conversion plate kept at a voltage of about −25 kV in order to achieve high detection efficiencies. The electrons emitted from the conversion plate are focused on a multi-channelplate detector and the fast timing signals are registered with a 'multihit' time to digital converter (TDC) on an event by event basis. The high impact energies of the clusters of fullerenes, fullerene monomers, and fragments at the conversion plate are needed in order to reach the high detection efficiencies, which are crucial to the multi-correlation studies of this, the second, experiment.

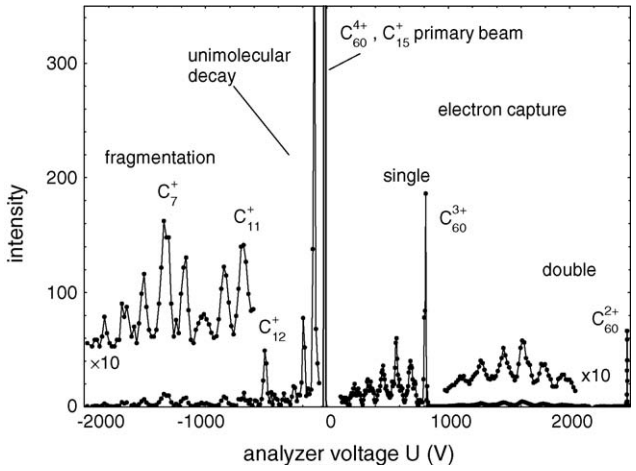


Fig. 1. Mass-to-charge spectrum of fragmented and intact fullerene projectiles measured at 0° for $C_{60}^{4+}$–$C_{60}$ collisions at 10 keV. The spectrum is obtained by changing the floating voltage $U$ of the energy analyzer (cf. text).

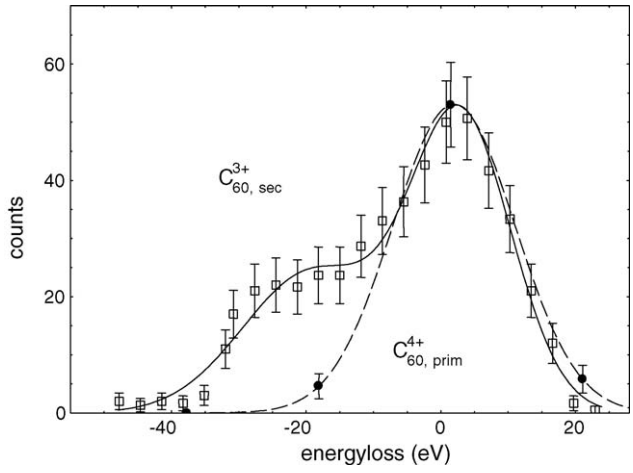


Fig. 2. Energy distribution of $C_{60}^{3+}$ projectile ions (open squares and full curve) formed by single-electron capture in $C_{60}^{4+}$–$C_{60}$ collisions at 0°. The full points and the dashed curve represent the energy profile of the primary $C_{60}^{4+}$ beam.

## 3. Results for $C_{60}^{q+}$–$C_{60}$ collisions

In Fig. 1, we show the projectile energy spectrum for 10 keV $C_{60}^{4+} + C_{60}$ collisions measured in the forward direction (0°) and with an angular acceptance of ±0.1°. This spectrum mainly represents a mass-to-charge spectrum of the projectile beam after the collision, as the energy exchange is rather small for peripheral collisions. The intensity of the primary peak ($C_{60}^{4+}$ at $U$, ∼0 V, where $U$ is the floating voltage of the energy analyzer) exceeds the full scale by roughly a factor of 2000, yielding a total reaction rate of the order of ∼1%. At positive voltages ($U > 0$ V), products of single ($C_{60}^{3+}$)- and double ($C_{60}^{2+}$)-electron capture are identified accompanied by 'evaporation series' yielding $C_{60-2m}^{r+}$ projectile ions with $r = 3$ and 2. To the left of the main peak, signals due to $C_{60-2m}^{4+}$ and small-sized fragments $C_n^+$ in the range $n = 4$–14 are observed. In the following, we will focus mainly on the production of the heavy fragments ($m/q > 15$) as the lighter ones may be due to collisions of the $C_{15}^+$ ions present in the primary beam.

### 3.1. Electron capture by the projectile in $C_{60}^{q+}$–$C_{60}$ collisions

As shown in Fig. 1, one or two electrons can be captured and stabilized by the $C_{60}^{4+}$ projectile yielding intact $C_{60}^{3+}$ and $C_{60}^{2+}$ projectile ions. Both peaks are rather narrow indicating that large impact parameters and low-energy transfers are involved. The single-electron capture peak ($C_{60}^{3+}$) shows a shoulder which extends to an energy loss of about 35 eV as is evident from the comparison with the energy profile of the primary $C_{60}^{4+}$ beam in Fig. 2. This energy loss, which is stored in the collision partners as vibrational energy, does obviously not cause fragmentation of the fullerene projectile. Closer collisions with larger energy transfers to the internal degrees of freedom (added to the initial internal energies of the fullerenes) are required to induce $C_2$-evaporation within the present experimental time scale of about 13 μs.

In addition to pure electron capture, there are other channels where capture is associated with the loss of an even number of C-atom. In the case of collisions between atomic ions and fullerenes, these features are well known and for low cluster charges they are attributed to the evaporation of neutral $C_2$ molecules. For the fullerene charge state $r = 4$, fission becomes competitive and is characterized by the emission of singly charged smaller-sized fragments (mainly $C_2^+$). At still higher fullerene charge states fission will dominate [28].

The fragment distribution for three times charged projectile ions ($C_{60-2m}^{3+}$) is shown in more detail in Fig. 3. The fragment peaks clearly have much larger energy spreads than the peak due to non-dissociated $C_{60}^{3+}$. This increase in widths is caused by the emission of low-energy $C_2$ or $C_2^+$ molecules in the rest frame of the projectile (kinematic effect), but also to the dynamics of the collision process. Similar broadenings are also found in the measured angular distributions of the individual peaks, which

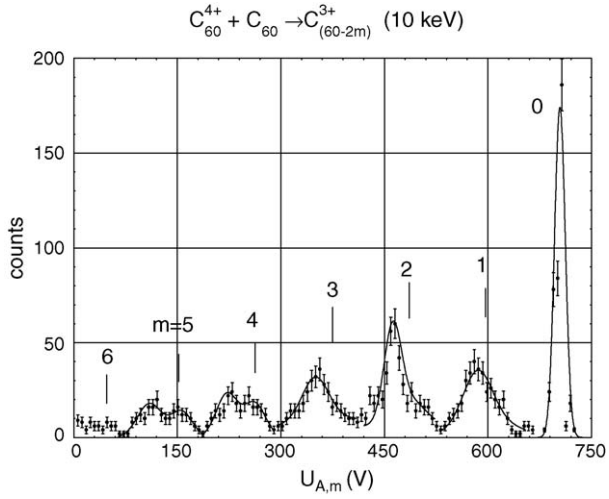


Fig. 3. Mass and energy distribution of $C_{60-2m}^{3+}$ ions ($m = 0$–5). The full curves correspond to Gaussian fit analysis. The vertical lines indicate the positions where the fragmented ions with the same velocities as the incident $C_{60}^{4+}$ projectile would be expected.

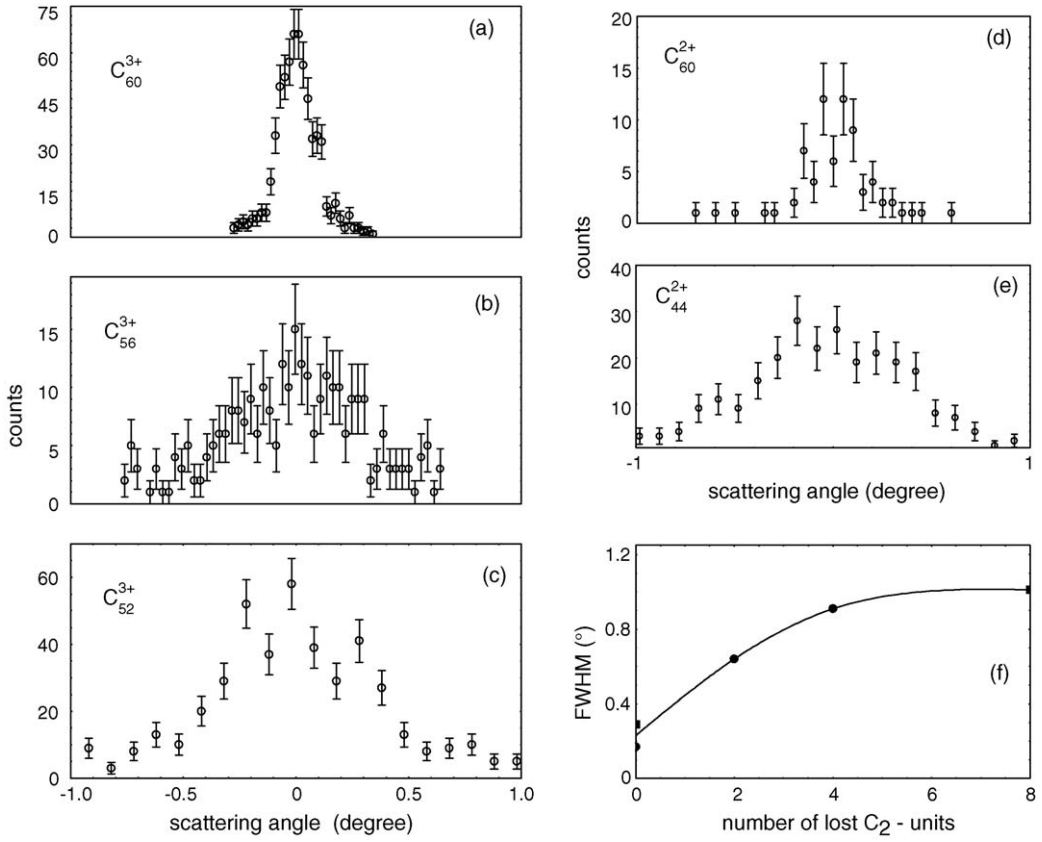


Fig. 4. (a)–(e) Angular distributions for the $C_{60}^{4+}$–$C_{60}$ product ions $C_{60}^{3+}$, $C_{56}^{3+}$, $C_{52}^{3+}$, $C_{60}^{2+}$, and $C_{44}^{2+}$, respectively. (f) The full width at half maximum of the angular distributions as a function of the number of lost $C_2$-unit. The full dots correspond to triply charged systems, whereas the full squares belong to the doubly charged ones.

are shown in Fig. 4. Whereas the projectile angular scattering distributions for intact $C_{60}^{3+}$- and $C_{60}^{2+}$-molecule are rather narrow, those associated with the losses of several C-atoms are much wider. Fig. 4f indicates that the half-widths of the angular distributions increase with the number of $C_2$-molecules lost from the projectile fullerene in a way which is independent of the final fragment charge state $r$. This finding can be understood as a consequence of the fact that decreasing impact parameters lead to larger energy transfers and thus to increased fragmentation.

We note from Fig. 3 that the positions of the measured fragment peaks are shifted towards lower energies with respect to fragments, which would have the same velocity as the incident $C_{60}^{4+}$ projectile (marked by vertical lines in Fig. 3). These energy differences give the energy losses of the residual projectile ions. In order to further discuss the observed peak forms, we have to take into account that two different processes may contribute. Either single-electron capture is followed by the evaporation of a neutral $C_2$ molecule or a charged $C_2^+$ ion is emitted directly in a unimolecular decay process.

The narrow peaks for the $(C_{60-2m})^{4+}$ ions on the left hand side of the primary peak in Fig. 1 indicate that unimolecular decay processes are important. In principle, these signals can either be due to collision-induced dissociation without charge transfer or due to the unimolecular decay of thermally excited projectiles. As shown in Fig. 5 (full squares), the $C_{60-2m}^{4+}$ ions are formed without any energy loss, independent of the number of emitted $C_2$ molecules, and hence they are attributed to unimolecular decay processes. The required activation energy of about 10 eV [29,30] per emitted $C_2$-unit indicates that the internal energy of the incident projectile, produced in the ECR ion source, is rather high. The strong intensity increase which seems to occur in the

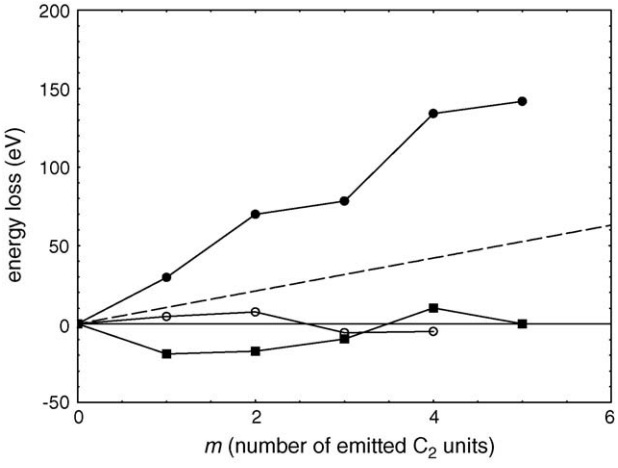


Fig. 5. Average energy losses in the unimolecular decay of $C_{60}^{4+}$ (loss of $m$ $C_2$-units, open circles), for single-electron capture associated with the loss of $m$ $C_2$-units (full circles), and the loss of $C_2^+$ (or $C4^+ \ldots$) ions from the $C_{60}^{4+}$ projectile (full squares). The dashed line indicates the energetic thresholds for sequential $C_2$ emission. The activation energy is taken to be 10 eV per $C_2$ molecule [29,30].

evaporation series for $m = 6$, corresponding to $C_{48}{}^{4+}$, is due to an overlapping $C_{12}{}^{+}$ fragment, originating from the fragmentation of contaminant $C_{15}{}^{+}$ projectiles, present in the primary beam.

When analyzing the peak forms in Fig. 3, two different contributions can be identified, in particular, when the number of lost $C_2$ molecules increases. The first type is characterized by a zero energy loss and is attributed to unimolecular fission (for example, emission of one $C_2{}^{+}$-molecule and $(m-1)$ neutral $C_2$ molecules), activated by the internal energies of the incident projectiles. The second process, giving slightly larger contributions to the fragment spectrum, gives peaks, which are shifted towards larger energy losses as the number of emitted $C_2$ molecules increases. The measured energy losses for unimolecular decay ($C_2$ emission from $C_{60}{}^{4+}$) and unimolecular fission ($C_2{}^{+}$ emission from $C_{60}{}^{4+}$) are shown as open circles and full squares in Fig. 5, respectively. For single-electron capture, the energy loss increases from 0 to about 140 eV as the number of lost $C_2$-units increases from $m = 0$ to 5 (full dots on Fig. 5). Taking the typical initial internal energy of the projectile ions into account, we arrive at internal energies, which are well above the activation energies for $C_2$ emission. The activation energy for (sequential) $mC_2$ emission is indicated with a dashed line in Fig. 5. These observations strongly indicate that the fragmentation associated with single-electron capture in $C_{60}{}^{4+}$–$C_{60}$ collisions is statistical in nature.

### 3.2. Recoil ions and particle coincidences

Under the given experimental conditions (with a weak recoil ion extraction field) only low-energy fullerene target ions from $C_{60}{}^{q+}$–$C_{60}$ collisions can be detected. Thus, products from closer collisions, in particular those causing fragmentation of the target, are strongly suppressed in the recoil spectrum. In Fig. 6, we compare the recoil ion spectrum obtained for two types of projectiles: $C_{60}{}^{4+}$ at 8 keV and $C^{4+}$ at 4 keV. Here we want to emphasize that the recoil ion spectrum for $C_{60}{}^{4+} + C_{60}$ collisions only shows intact fullerenes and, further, that these fullerenes are only found in charge states 1+ and 2+. In the case of atomic ions (lower part of Fig. 6), intact recoil ions in all charge states up to the limit of the initial projectile charge (4+) are observed. Similar differences are observed for all projectile charge states between $q = 2$ and 5: atomic ions can ionize the $C_{60}$ target up to the initial projectile charge $q$ [31], whereas fullerene projectiles lead to a maximum recoil charge of $r_{max} = q/2$ for even values of $q$ and $r_{max} = (q+1)/2$ for odd $q$. This means that the projectile charge is equally distributed on the projectile and the target fullerene for even $q$ and for sufficiently close $C_{60}{}^{q+} + C_{60}$ collisions on a time scale which must be shorter than the 10 fs collision time.

In a simple model, in which the fullerene molecules are treated as conducting spheres [32,33] the observed charge separation effect is a consequence of the symmetry of the collision system and of the high mobility of charges between the spheres (fullerenes) at sufficiently small separations. We define the total cross section for electron removal as, $\sigma_{tot} = \pi(R_1^2 - b_{max}^2)$ where $b_{max}$ is the maximum impact parameter for target fragmentation (collisions with smaller impact parameters cannot be detected in the coincidence experiment) and $R_1$ the critical distance for the transfer of the outermost target electron. In a similar way, the cross section for removing $r$ electrons is defined as $\sigma_r = \pi(R_r^2 - R_{r+1}^2)$. In Fig. 7, we compare the calculated and the experimental [27] relative cross sections ($\sigma_r/\sigma_{tot}$) for $[C_{60}{}^{q+} + C_{60}]$ and $[C^{q+} + C_{60}]$ collisions at the velocities $v = 0.01q^{1/2}$ and $0.06q^{1/2}$ a.u., respectively. The critical distances for electron removal, which have been calculated, using the model described in Refs. [32,33], are shown in Table 1. In the calculations the fullerene radius was set to $8.37a_0$ as deduced from the classical relation between the radius of a conducting sphere [32] and the sequence of recently calculated $C_{60}$ ionization potentials [34]. The radius of the $C^{q+}$ projectile was set to zero in the present model calculations. For the odd fullerene projectiles, we have taken into account the charge division effect by dividing the cross section by 2 for the last electron transfer ($r = r_{max}$), thus, $\sigma_{r_{max}} = \pi(R_{r_{max}}^2 - b_{max}^2)/2$. As a consequence, the cross sections for removing $(r_{max} - 1)$ electrons have been increased by the corresponding amounts for odd $q$. The maximum impact parameter for target fragmentation was determined semi-empirically by fitting the $\sigma_{r_{max}}$ values for $q = 5$, yielding $19.7a_0$ and $12.9a_0$ for

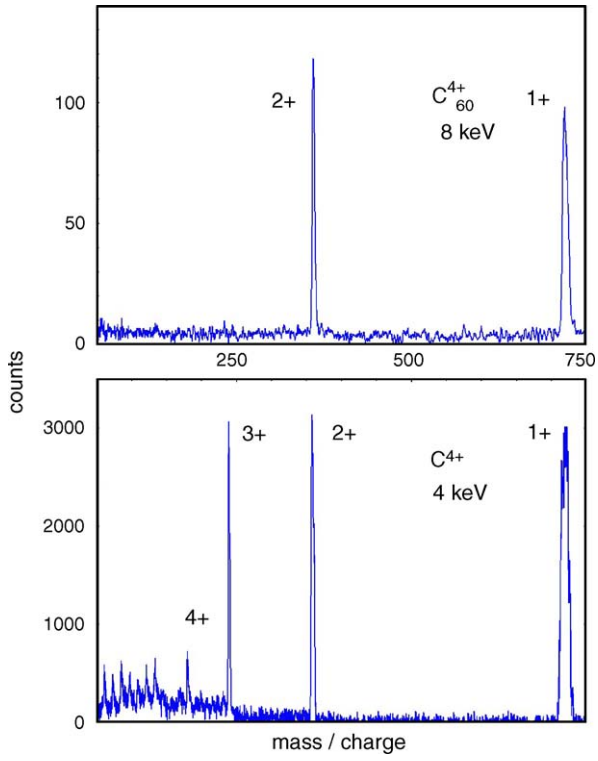


Fig. 6. Mass/charge spectrum showing the recoil ion distribution produced in $C_{60}{}^{4+} + C_{60}$ collisions at 8 keV (upper part), and $C^{4+} + C_{60}$ collisions at 4 keV (lower part).

Table 1
Critical distances for electron transfer in $C_{60}{}^{q+}$–$C_{60}$ collisions given in atomic units

| $q$ | 2 | 3 | 4 | 5 |
|---|---|---|---|---|
| $R_1$ | $20.9a_0$ | $21.7a_0$ | $22.3a_0$ | $24.2a_0$ |
| $R_2$ | | $20.2a_0$ | $20.8a_0$ | $21.6a_0$ |
| $R_3$ | | | | $20.2a_0$ |

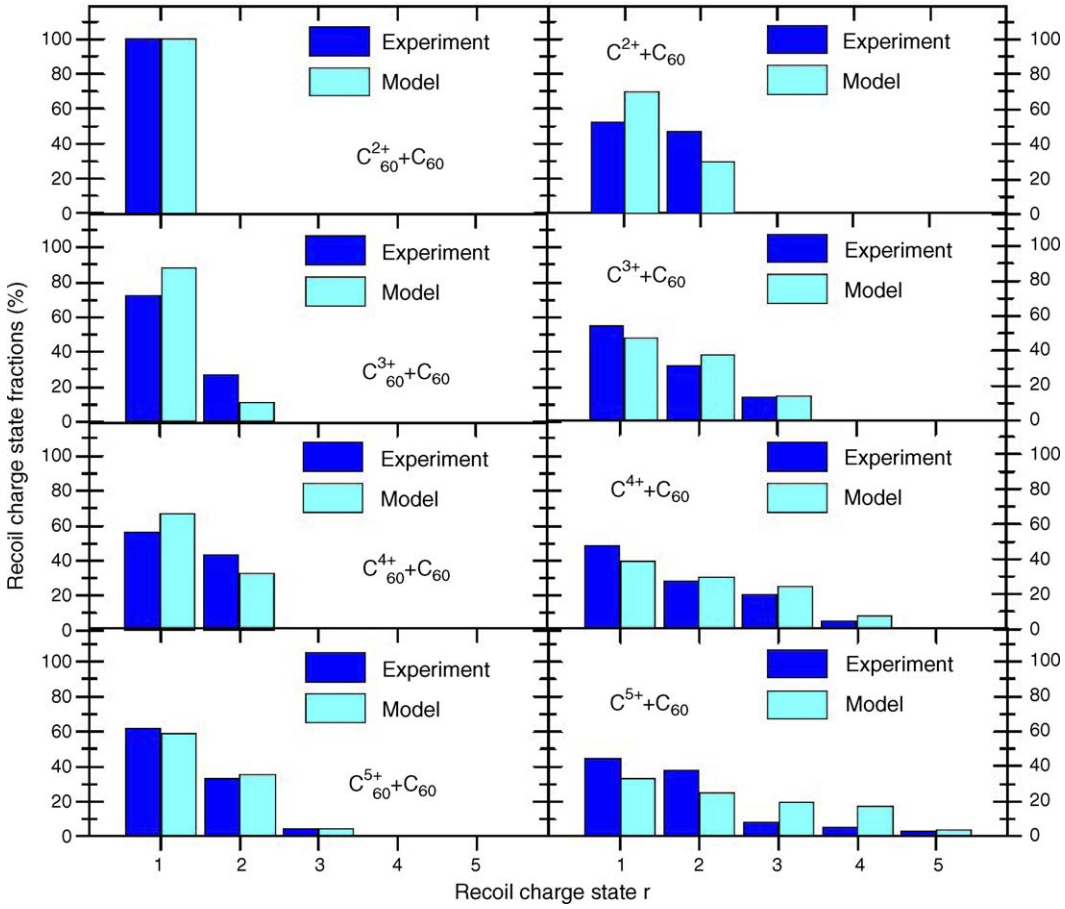


Fig. 7. Relative charge state fractions in non-fragmenting $C_{60}{}^{q+} + C_{60}$ (left column) and $C^{q+} + C_{60}$ collisions (right column).

the fullerene and (atomic) carbon projectiles, respectively. The agreement between the model calculations and the experimental values are surprisingly good, not only with respect to the number of possibly transferred electrons but also concerning the partial cross sections for transfers of *r* electrons. This indicates that the simple model is well adapted to describe the essentials of the underlying charge-exchange mechanisms.

The 10 keV $C_{60}{}^{q+} + C_{60}$ recoil coincidence spectra for stabilization of one and two electrons on the projectile are shown in comparison with the corresponding results for 7.6 keV

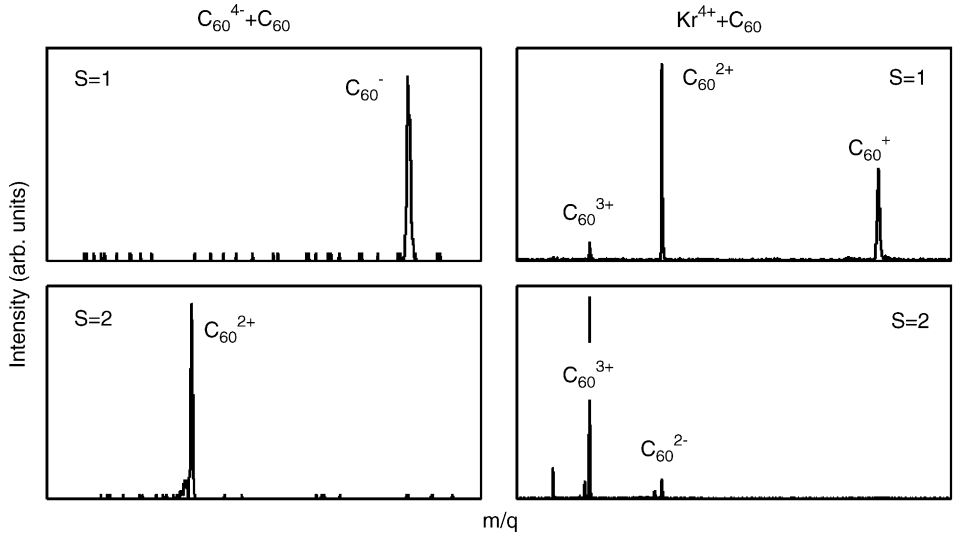


Fig. 8. Recoil ion mass spectra registered in coincidence with one (upper part) and two (lower part) electrons stabilized on the projectile in 10 keV $C_{60}{}^{4+} + C_{60}$ (left) and $Kr^{4+} + C_{60}$ (right) collisions. The projectile ions were measured at a scattering angle of $(0 \pm 0.1)^\circ$.

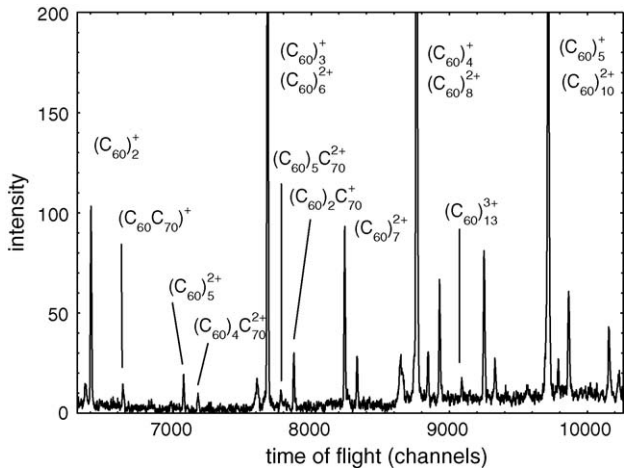


Fig. 9. Time-of-flight spectrum showing the range of small clusters of fullerenes in different charge states, obtained in collisions of $Xe^{30+}$ ions with $(C_{60})_n$ at 600 keV.

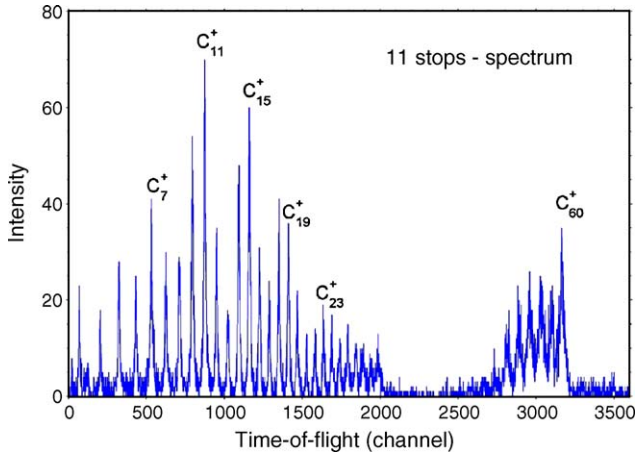


Fig. 10. Time-of-flight spectrum constructed from those events, where 11 charged particles have been detected (11-stop spectrum). Collision system: $Xe^{30+} + C_{60}$ at 600 keV.

$Kr^{4+} + C_{60}$ collisions in Fig. 8. Here, we note that only singly charged recoil ions are observed for $s = 1$ (one electron stabilized on the projectile) when fullerene projectiles are used, while up to triply charged recoil ions are seen for $s = 1$ with $Kr^{4+}$ projectiles. Thus, no transfer ionization events occur in the fullerene projectile case, i.e., the formation of doubly or triply excited states on the projectile with sufficient excitation energies to cause electron emission is unlikely to occur. Furthermore, the doubly charged peaks for $s = 2$ originate from true double electron capture and also here there is no emission of electrons. At a first glance the absence of transfer ionization is very surprising as these processes are known to be very important for slow atomic collisions with multiply charged (atomic) projectile ions, as can be seen in the results for $Kr^{4+} + C_{60}$ collisions shown to the right in Fig. 8. However, the differences between the spectra can be explained within the over-the-barrier conducting sphere model of Zettergren et al. [32]. The total projectile excitation energy after the transfer of two electrons from one model conducting sphere (the target $C_{60}$) to the other conducting sphere (the projectile $C_{60}{}^{4+}$) is 7.8 eV [33], which is considerably smaller than the ionization energy for the doubly charged fullerene (16.9 eV [21]). Therefore, the transfer ionization channel is closed for simple energetic reasons in $C_{60}{}^{4+} + C_{60}$ collisions.

## 4. Clusters of fullerenes

Clusters of fullerenes, containing up to 40 molecules of $C_{60}$ (and $C_{70}$ — there is an admixture of 1:20 of $C_{70}$ in the powder), are multiply ionized in slow collisions with highly charged atomic projectile ions ($Xe^{30+}$ at 600 keV). A part of a typical mass spectrum, showing the range of singly and multiply charged clusters, either ionized directly without fragmentation or stemming from fragmenting larger clusters, is shown in Fig. 9. This type of spectrum has been analyzed before with respect to geometrical shell effects and so-called appearance sizes, which are the smallest sizes for given charge states which are observed in the mass spectrum [11–13]. In particular, it has been shown that the smallest doubly charge cluster is the pentamer $(C_{60})_5{}^{2+}$.

Concerning the charge mobility in van der Waal's type fullerene clusters, it is useful to start out by considering the smaller systems, i.e., the fullerene dimers and trimers, which are present in the spectrum as singly charged ions. However, they are evidently unstable when a second charge is added (these ions are thus not directly observed in the overall time-of-flight spectrum but the correlated fragmentation products may be identified by using the multi-stop coincidence spectra). The neutral $C_{60}$ dimer, $(C_{60})_2$, is known to be bound by about 0.3 eV and has an equilibrium distance of 19.0 $a_0$ according to the Girifalco potential [35], commonly used for the description of the van der Waal's type interaction between neighboring monomers in fullerene-based materials. If we add one charge to one of the $C_{60}$ molecules in the dimer and use the model of two interacting conducting spheres [32] we find that the binding energy increases to about 0.4 eV, which is close to the only existing experimental value [15]. The addition of one charge does not change the equilibrium distance by any appreciable amount and it is noted that the equilibrium distance in the $(C_{60})_2{}^+$ dimer is considerably smaller than the outermost critical distance for electron transfer between the spheres (see Table 1). This readily explains why the charges in a cluster of $C_{60}$ molecule are highly mobile as soon as $(C_{60})_n$ is singly charged.

A further evidence of high charge mobility is deduced from the measured fragmentation patterns of larger clusters which are multiply charged before fragmentation. A typical spectrum which contains only events where 11 charged particles have been detected is shown in Fig. 10. This means that in this case large clusters have been ionized at least 11 times. The spectrum shows only singly charged fragments: small singly charged carbon clusters and singly charged fullerene molecules of which some have lost one or several $C_2$ molecules. Thus, the cluster which is initially eleven times charged breaks apart into eleven singly charged fragments and the initial charge must have been well distributed within the cluster before fragmentation. The distribution and the peak widths of the small-sized fragments

rather correspond to a thermally activated fragmentation process than to a charge-driven fragmentation of individual $C_{60}$ molecules.

## 5. Summary

In the experimental study of $C_{60}^{q+}$–$C_{60}$ collisions we have shown that sufficiently close, non-fragmenting collisions lead to an equal distribution of the charge on the two molecules for even $q$. For odd fullerene projectile charge states, the maximum final target fullerene charge is found to be $(q+1)/2$. We have further shown that these charge redistribution processes occur on time scales shorter than the collision time, which is of the order of 10 fs. These results could be rationalized by means of an earlier published model for over-the-barrier electron transfer between two conducting spheres. The same model is also used to calculate excitation energies following electron transfer between two fullerenes. The calculated low values explain the present observation that transfer ionization processes are *fully suppressed* for $C_{60}^{q+}$–$C_{60}$ collisions in the present charge state range ($q = 2$–5). At a first glance this appeared to be surprising as transfer ionization processes in which a number of electrons are transferred to the projectile in a first step followed by autoionization of a multiply excited projectile state play an important role for atomic ions of the same charge states colliding with $C_{60}$. This has been clearly demonstrated also in the present work.

Single-electron capture in $C_{60}^{4+}$–$C_{60}$ collisions, sufficiently close to induce fragmentation of the fullerene projectile, were found to be associated with energy losses that increased rather strongly with the number of emitted $C_2$-units reaching energy losses of about 140 eV for the $C_{50}^{3+}$ projectile fragments. Taking also the initial excitation of the incident $C_{60}^{4+}$ projectile into account, the total internal energies are sufficiently high to strongly suggest that the fragmentation processes associated with single-electron capture are statistical.

Using the results of the $C_{60}^{q+}$–$C_{60}$ collision experiment and the agreement with the result of the classical over-the-barrier model, we argue that the high charge mobility which we have established for ionized clusters of fullerenes may be understood through a very simple basic argument: the critical distance for over-the-barrier electron transfer in the $C_{60}^{+}$–$C_{60}$ system is larger than the equilibrium distance in the $(C_{60})^{2+}$ van der Waal's dimer system. As the $C_{60}$–$C_{60}$ distances are similar in the clusters of fullerenes and in the dimers, we conclude that the charge may "hop" from one molecule to another as soon as it becomes singly charged. The hopping time is most likely shorter than 10 fs.

## Acknowledgments

Some of the experiments have been performed at the 'ARIBE' facility at GANIL. This work has been initiated under the European network LEIF (HPRI-CT-1999-40012). PH and ST thank the Danish National Research Foundation through the Aarhus Center for Atomic Physics (ACAP). This work was also supported by the Swedish Natural Science Research Council and by the Swedish Foundation for International Cooperation in Research and Higher Education (STINT).

## References

[1] H. Cederquist, A. Fardi, K. Haghighat, A. Langereis, H.T. Schmidt, S.H. Schwartz, J.C. Levin, I.A. Sellin, H. Lebius, B. Huber, M.O. Larsen, P. Hvelplund, Phys. Rev. A 61 (2000) 022705.
[2] H. Zettergren, J. Jensen, H.T. Schmidt, H. Cederquist, EPJD 29 (2004) 63.
[3] S. Martin, R. Brédy, J. Bernard, J. Désesquelles, L. Chen, Phys. Rev. Lett. 89 (2002) 183401.
[4] S. Martin, L. Chen, R. Brédy, J. Bernard, A. Salmoun, B. Wei, Phys. Rev. A 69 (2004) 043202.
[5] J. Jensen, H. Cederquist, H. Zettergren, H.T. Schmidt, S. Tomita, S.B. Nielsen, J. Rangama, P. Hvelplund, B. Manil, B.A. Huber, Phys. Rev. A 69 (2004) 053203.
[6] H. Shen, P. Hvelplund, D. Mathur, A. Barany, H. Cederquist, N. Selberg, D.C. Lorents, Phys. Rev. A 52 (1995) 3847.
[7] E.E.B. Campbell, V. Schyja, R. Ehlich, I.V. Hertel, Phys. Rev. Lett. 70 (1993) 263.
[8] F. Rohmund, A. Glotov, K. Hansen, E.E.B. Campbell, J. Phys. B: Atom. Mol. Opt. Phys. 29 (1996) 5163.
[9] A.V. Glotov, E.E.B. Campbell, Phys. Rev. A 62 (2000) 033202.
[10] O. Knospe, R. Schmidt, in: J. Jellinek (Ed.), Theory of Atomic and Molecular Clusters, Sringer Series on Mesoscopic Phenomena, Sringer, 1997.
[11] B. Manil, L. Maunoury, B.A. Huber, J. Jensen, H.T. Schmidt, H. Zettergren, H. Cederquist, S. Tomita, P. Hvelplund, Phys. Rev. Lett. 91 (2003) 215504.
[12] B. Manil, L. Maunoury, J. Jensen, H. Cederquist, H.T. Schmidt, H. Zettergren, P. Hvelplund, S. Tomita, B.A. Huber, Nucl. Instrum. Meth. Phys. Res. B 235 (2005) 419.
[13] B. Manil, P. Boduch, A. Cassimi, O. Kamalou, L. Maunoury, J. Rangama, J. Jensen, H. Zettergren, H. Cederquist, B.A. Huber, Int. J. Mod. Phys. B 19 (15–17) (2005) 2345.
[14] T.P. Martin, U. Näher, H. Schaber, U. Zimmermann, Phys. Rev. Lett. 70 (1993) 3079.
[15] W. Branz, N. Malinowski, A. Enders, T.P. Martin, Phys. Rev. B 66 (2002) 094107.
[16] W. Branz, N. Malinowski, H. Schaber, T.P. Martin, Chem. Phys. Lett. 328 (2000) 245.
[17] J.P.K. Doye, D.J. Wales, W. Brantz, F. Calvo, Phys. Rev. B 64 (2001) 235409.
[18] K. Hansen, R. Müller, H. Hohmann, E.E.B. Campbell, Z. Phys. D 40 (1997) 361.
[19] M. Hedén, K. Hansen, E.E.B. Campbell, Phys. Rev. A 71 (2005) 055201.
[20] J.C. Hummelen, B. Knight, J. Pavlovich, R. Gonzàles, F. Wudl, Science 269 (1995) 1554.
[21] K. Lee, H. Song, B. Kim, J.T. Park, S. Park, M.-G. Choi, J. Am. Chem. Soc. 24 (2002) 2872.
[22] See for example:.See for example: R.L. Johnston, in: D.S. Betts (Ed.), Atomic and Molecular clusters, Masters Series In Physics and Astronomy, Taylor & Francis, 2002.
[23] W. Tappe, R. Flesch, E. Rühl, R. Hoekstra, T. Schlathölter, Phys. Rev. Lett. 88 (2002) 143401.
[24] J. Opitz, H. Lebius, B. Saint, S. Jacquet, B.A. Huber, H. Cederquist, Phys. Rev. A 59 (1999) 3562.
[25] L. Maunoury, B. Manil, J. Rangama, H. Lebius, B.A. Huber, J.Y. Pacquet, R. Leroy, U.V. Pedersen, P. Hvelplund, J. Jensen, S. Tomita, H. Zettergren, H.T. Schmidt, H. Cederquist, Rev. Sci. Instrum. 76 (2005) 053304.
[26] F. Chandezon, S. Tomita, D. Cormier, P. Grübling, C. Guet, H. Lebius, A. Pesnelle, B.A. Huber, Phys. Rev. Lett. 87 (2001) 153402.
[27] H. Cederquist, P. Hvelplund, H. Lebius, H.T. Schmidt, S. Tomita, B.A. Huber, Phys. Rev. A 63 (2001) 025201.

[28] S. Martin, L. Chen, A. Denis, J. Desesquelles, Phys. Rev. A 57 (1998) 4518.
[29] S. Tomita, J.U. Andersen, C. Gottrup, P. Hvelplund, U.V. Pedersen, Phys. Rev. Lett. 87 (2001) 0734011.
[30] S. Diaz-Tendero, M. Alcami, F. Martin, Phys. Rev. Lett. 95 (2005) 013401.
[31] This statement is valid for low charge states. In the case of highly charged ions, for example $Xe^{30+}$, a much larger number of electrons can be released (of the order of 100).
[32] H. Zettergren, H.T. Schmidt, H. Cederquist, J. Jensen, S. Tomita, P. Hvelplund, H. Lebius, B.A. Huber, Phys. Rev. A 66 (2002) 032710.
[33] H. Zettergren, Ph.D. thesis, Department of Physics, Stockholm University, 2005.
[34] S. Díaz-Tendero, M. Alcamí, F. Martín, Phys. Rev. Lett. 95 (2005) 013401.
[35] L.A. Girifalco, J. Phys. Chem. 96 (1992) 858.